Available on-line at www.prace-ri.eu

Partnership for Advanced Computing in Europe

Generating Massive Unstructured Meshes for OpenFOAM

Seren Soner[a], Can Özturan[a,*]

[a]Computer Engineering Department, Bogazici University, Istanbul, Turkey

Abstract

OpenFOAM is an open source computational fluid dynamics (CFD) package with a large user base from many areas of engineering and science. This whitepaper documents an enablement tool called PMSH that was developed to generate multi-billion element unstructured tetrahedral meshes for OpenFOAM. PMSH is developed as a wrapper code around the popular open source sequential Netgen mesh generator. Parallelization of the mesh generation process is carried out in five main stages: (*i*) generation of a coarse volume mesh (*ii*) partitioning of the coarse mesh to get sub-meshes, each of which is processed by a processor (*iii*) extraction and refinement of coarse surface sub-meshes to produce fine surface sub-meshes (*iv*) re-meshing of each fine surface sub-mesh to get the final fine volume mesh (*v*) matching of partition boundary vertices followed by global vertex numbering. An integer based barycentric coordinate method is developed for matching distributed partition boundary vertices. This method does not have precision related problems of floating point coordinate based vertex matching. Test results obtained on an SGI Altix ICE X system with 8192 cores and 14 TB of total memory confirm that our approach does indeed enable us to generate multi-billion element meshes in a scalable way. PMSH tool is available at https://code.google.com/p/pmsh/.

1. Introduction

We developed an enablement tool called PMSH for facilitating the fast generation of unstructured multi-billion element tetrahedral meshes (grids) on complex geometries for the OpenFOAM computational fluid dynamics (CFD) package [1]. PMSH is developed as a C++ wrapper code around the popular open source sequential Netgen mesh generator [2]. OpenFOAM provides a mesh generator called blockMesh for simple geometries. The blockMesh utility is a multi-block mesh generator that generates hexahedral meshes from a text configuration file. For complex geometries, OpenFoam also provides a mesh generation utility called snappyHexMesh which generates hexahedral meshes. The snappyHexMesh utility works more like a mesh sculptor rather than a generator. It takes an existing mesh such as the one produced by blockMesh and chisels out a mesh on a complex geometry that is given in STL format. The snappyHexMesh utility has advanced features like the ability to run in parallel and being able to redistribute the mesh so as to perform automatic load balancing. Both utilities, snappyHexMesh and blockMesh, are not as advanced as other commercial or open source mesh generator packages for producing quality tetrahedral meshes on complex geometries. Therefore, there is a great need in the OpenFOAM community for tools that will enable researchers to generate massive meshes on complex geometries.

Löhner states in [3] that *"grid sizes have increased by an order of magnitude every 5 years and that presently, grids in of the order of* 10^9 *elements are commonly used for leading edge applications in the aerospace, defense, automotive, naval, energy and electromagnetics sectors"*. Löhner also mentions that *"for applications where remeshing is an integral part of simulations, e.g. problems with moving bodies or changing topologies, the time required for mesh regeneration can easily consume a significant percentage of the total time required to solve the problem"*. Geometry and mesh generation related concerns have also been voiced in a recent Applied Mathematics for Exascale Report [4] by the U.S. based Exascale Mathematics Group. Therefore, as we move towards exascale computing, the ability to generate massive multi-billion meshes especially on complex geometries will be in more demand in the future.

*Corresponding author.
tel. +90-212-359-7225 fax. +90-212-387-2461 e-mail. ozturaca@boun.edu.tr

This whitepaper is organized as follows: Section 2 reviews the previous work done in the area of mesh generation and refinement. Section 3 presents the details of our algorithms and data structures used. Section 4 lists modifications that needed to be done in order to fix some bugs in Netgen. Section 5 presents the results of various parallel mesh generation tests we have carried out on an SGI Altix ICE X system with 8192 cores. Finally, conclusions and future work are presented in Section 6.

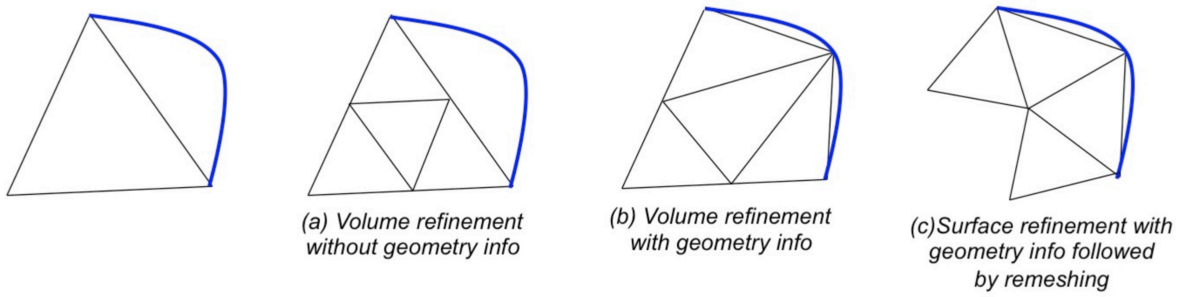
(a) Volume refinement without geometry info
(b) Volume refinement with geometry info
(c)Surface refinement with geometry info followed by remeshing

Fig. 1: Given a coarse mesh volume refinements of the mesh without (a) or with (b) geometry information and remeshing after surface refinement with geometry information (c)

2. Previous Work

Parallel mesh generation has been addressed in several reported works: Dawes *et al.* [5] presents bottom up octree based parallel mesh generation routines. Blagojevic *et al.* [6] parallelizes Delaunay based mesh generation on multicore SMT-based architectures. D3D [7] is an MPI based parallel mesh generator that employs octree based mesh generation. MeshSim by Simmetrix Inc. is a commercial multi-threaded and distributed parallel mesh generator [8]. ParTGen [9] is a parallel mesh generator that uses a geometry decomposition based approach to decouple the meshing process into parallel mesh generation tasks. Performance tests of PartTgen have demonstrated scalability only up to 32 processors. The approach taken in PMSH is similar to that of ParTgen.

The work by Löhner [3] is a very recent work involving geometry decomposition and the use of advancing front technique on multiple sub-domains to generate meshes in parallel. It is reported that billion element sized meshes have been generated in roughly forty minutes on a 512 core SGI ITL machine.

Pamgen [10] is another parallel mesh generation library within the Trilinos Project that produces hexahedral or quadrilateral meshes of simple topologies. It is stated in its FAQ page that the number of elements PAMGEN can generate is limited to just above two billions (because of 32 bit integer limitation).

Figure 1 illustrates refinement based approaches that can be used to generate massive meshes. Uniform mesh refinement without the use of geometric information, as shown in (a), works very fast in parallel, is quite scalable to tens of thousands of processors and can be used to produce meshes with tens of billions of elements. The works by Houzeaux *et al.* [11], Kabelikova *et al.* [12, 13] can be shown as examples of uniform refinement. These approaches, however, cannot be used on problems involving complex geometries with curved boundaries. In such cases, they cannot accurately approximate the boundary of the geometry. An alternative method is to do uniform refinement but also make use of geometric information as shown in Figure 1(b). This is the approach taken by Yilmaz *et al.* [14]. In this case, in addition to the mesh entities, one needs to have access to the geometry. Such an implementation can be achieved by utilizing mesh generation libraries as e.g. Netgen which is used in [14]. One and a half billion element meshes have been generated in this way in one to two minutes time on one thousand cores. Yilmaz *et al.* also provides results for a method involving decomposition of geometry in the flavour of Figure 1(c), where meshing of decomposed geometry is performed. However, geometry decomposition into a large number of sub-geometries introduces problems caused by thinly cut sub-domains. Using this method, meshes of about a few hundred million elements could be accomplished on up to 64 cores on simple geometries. A preliminary implementation was also reported in [14], which generates from a geometry a surface mesh, refines the surface mesh and generates a fine mesh from it in the style of Figure 1(c). This implementation had some problems and some preliminary results involving generation of a few million element meshes on few tens of cores were reported.

In our current PMSH work, the approach shown in Figure 1(c) involving generation of a coarse mesh, extraction of a surface mesh and re-meshing from a refined and projected fine surface mesh has been completely redesigned using new data structures and has been successfully implemented. The resulting implementation is robust and enabled us to generate multi-billion meshes on up to eight thousand processors (note that 8K processor is not a limitation of our PMSH but rather it was the maximum number of cores for the maximum allowable memory we could get on the specific supercomputer that we used for our tests). Also, note that both our PMSH and Löhner's work [3] employ a similar approach with Löhner using their own internal mesh generator and PMSH using the external Netgen mesh generator augmented with extra PMSH data structures, routines and modified Netgen libraries.

3. PMSH Parallel Mesh Generation Algorithm

Our mesh generation algorithm proceeds in five main stages: (*i*) Generation of a coarse volume mesh, (*ii*) Partitioning of the coarse mesh to get sub-meshes, each of which will be processed by a processor, (*iii*) Extraction and refinement of coarse surface sub-meshes to produce fine surface sub-meshes, (*iv*) Re-meshing of each fine surface sub-mesh to get the final fine volume mesh and (*v*) Matching of distributed duplicate partition boundary vertices followed by global vertex numbering.

Table 1: List of main symbols and their definitions

Symbol	Meaning
P	Number of processors (subdomains)
Ω	Closed geometric domain to be meshed
$\partial\Omega$	Boundary (surface) of geometry Ω
$\mathcal{T}$	Tetrahedral mesh
$\mathcal{T}^f$	Faces of tetrahedral mesh
$\mathcal{T}^v$	Vertices of tetrahedral mesh
$\partial\mathcal{T}$	Boundary of tetrahedral mesh
$\mathcal{T}_i$	Tetrahedral submesh (partitioned mesh) on processor i
$\partial\mathcal{T}_i$	Boundary of tetrahedral submesh (partitioned mesh) on processor i
$\mathcal{T}_i$	Faces of tetrahedral submesh (partitioned mesh) on processor i
r	number of refinement levels
$[(i,\alpha),(j,\beta),(k,\gamma)]$	Integer based global barycentric IDs where i,j,k are either 0 or indices of vertices from $\partial\mathcal{T}^v$ with $\alpha+\beta+\gamma=2^r$ and $i<j<k$

Given the list of symbols and their definitions in Table 1, Figure 2 presents the detailed steps of our parallel mesh generation algorithm. Steps 2-4 basically correspond to stage (*i*) that involves generation of an initial coarse mesh. Firstly, the geometry description Ω is loaded. Geometry file can be in STL or Netgen's CSG (.geo) format. A coarse mesh is then generated from this geometry. The coarse mesh basically enables us to subdivide our domain into P subdomains in a load balanced way.

In step 5, corresponding to stage (*ii*), version 5.1.0 of METIS [15] partitioner is used to partition the coarse mesh in a face-connected way. The coarse volume mesh and its partitioning is available on all the processors and hence allows each processor to compute processor adjacencies independently. In our current implementation, we let each processor to generate the coarse volume mesh and its partitioning redundantly. Even though energy and resources can be saved if a dynamic malleable job model is used (i.e. starting with a single processor and increasing the number of allocated processors after step 5), there are some complications involving reconstruction of Netgen's internal data structures on dynamically spawned processors. Therefore, we did not have time to address this malleable job model in this work.

Steps 6-9 correspond to stage (*iii*), which involves extraction and refinement of the coarse surface sub-mesh to produce a fine surface sub-mesh. Faces which are on the geometric boundary and faces which are shared by elements that are on different processors are extracted and a coarse surface sub-mesh is formed. This surface sub-mesh is then refined uniformly r times to form a fine sub-mesh. Refinement is done by our own code and not by Netgen code. A queue of faces to be refined is maintained. A face to be refined is pushed into this queue. After refinement, if it is to be refined again (i.e. $r-1$ more times), the newly created faces are also pushed into the queue. Using Netgen's library, newly formed vertices are projected onto the actual geometry boundary as part of step 9. Currently projection works only when meshing Netgen's CSG (.geo) geometry files. It does not work properly for STL geometries because sometimes Netgen's projection routine returns incorrect projections for some points.

Since we need to match new surface vertices with their counterparts on the neighbouring processors later on, we need to keep track of the addresses of newly created vertices. Our own refinement code helps us to do this tracking. We know the IDs of the coarse mesh vertices, since the same coarse mesh is present on all processors. The newly created vertices, however, have local IDs on each processor and these are different from

```
1: On all processors $i = 0 \dots P-1$ do
2:    Load geometry $\Omega$
3:    Generate coarse surface mesh $\partial\mathcal{T}$ for $\Omega$
4:    Generate coarse volume mesh $\mathcal{T}$
5:    Partition the coarse volume mesh $\mathcal{T}$ into $P$ parts $\mathcal{T}_i$, $i = 0 \dots P-1$
6:    Extract coarse surface mesh faces $\partial\mathcal{T}_i^f$ for all partitions $i = 0 \dots P-1$
7:    Construct surface mesh $\partial\mathcal{T}_i'$ from $\partial\mathcal{T}_i^f$
8:    Perform $r$-level refinement of surface mesh $\partial\mathcal{T}_i'$ to get fine surface
      mesh $\partial\mathcal{T}_i''$ and record barycentric global IDs of each newly created
      vertex
9:    Project new surface vertices in $\partial\mathcal{T}_i''$ to the geometric boundary $\Omega$
10:   Compute partition boundary vertex adjacencies to adjacent processors by using a map that uses barycentric global IDs as keys
11:   Generate fine volume mesh $\mathcal{T}_i''$ from the fine surface mesh $\partial\mathcal{T}_i''$
12:   Compute owners of partition boundary vertices held by adjacent processors (called holders)
13:   Compute global integer IDs of owned vertices
14:   Inform global integer IDs of the owned vertices to the holder processors by using barycentric global IDs as keys to locate the corresponding vertices on adjacent holder processors
15:   Output fine volume mesh $\mathcal{T}_i''$ in OpenFOAM format
16: enddo
```

Fig. 2: PMSH parallel mesh generation algorithm

their counterparts on other processors. Even though one can always use x, y, z coordinates of these vertices to match them, such a method uses floating point comparisons and can be sensitive to precision related errors. The generation of new vertices is done in different orders on different processors. Since multi-billion element meshes are to be generated, precision related problems are more likely to happen due to very small element sizes. As a result, we wanted to come up with a new integer based vertex identification system.

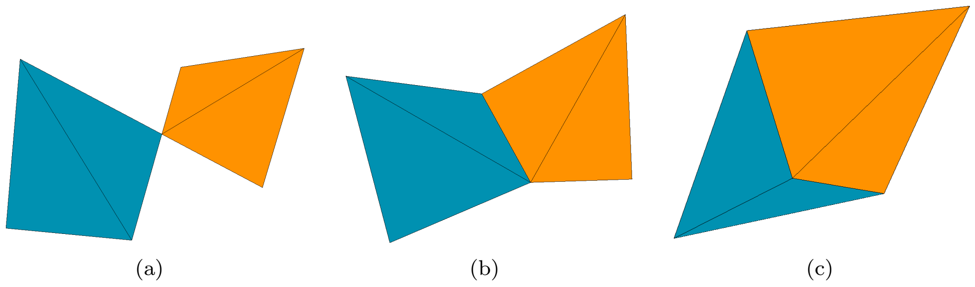

Fig. 3: Connectivity types ; vertex (a), edge (b) and face (c) connectivities

The new vertex identification system we came up with makes use of integer barycentric coordinates. All processors know the IDs of the coarse mesh vertices. Hence, given a coarse surface mesh face that is defined with vertices having indices i, j and k, the address of this face can be easily identified by employing a map that maps the key (i, j, k) to the corresponding local face address on each processor. However, when new faces and vertices are created as a result of refinement, their orders of creation are different on each processor. There can be different connectivity types as shown in Figure 3. Vertex connectivity is easy to resolve since the vertex connectivities of partitions can be established by the coarse mesh vertices which are known by all processors. The newly created vertices on edges and faces introduce complications because their orders of creation are different. Integer based barycentric coordinates help us to address all three types of connectivities and identify all types of vertices (coarse or newly created) by a single mechanism. We define barycentric global IDs as a sorted sequence of three (*vertex id, integer barycentric coordinate*) pairs, i.e., as $[(i,\alpha),(j,\beta),(k,\gamma)]$. Here, i, j, k are either 0 or indices of vertices from $\partial\mathcal{T}^v$ satisfying $i < j < k$ and α, β, and γ are integer barycentric coordinates with $\alpha + \beta + \gamma = 2^r$. Figure 4 shows an example of face defined by coarse mesh vertices 3, 5 and 8 and the newly created vertices as a result of 2-level refinement. The table in Figure 4 shows the barycentric

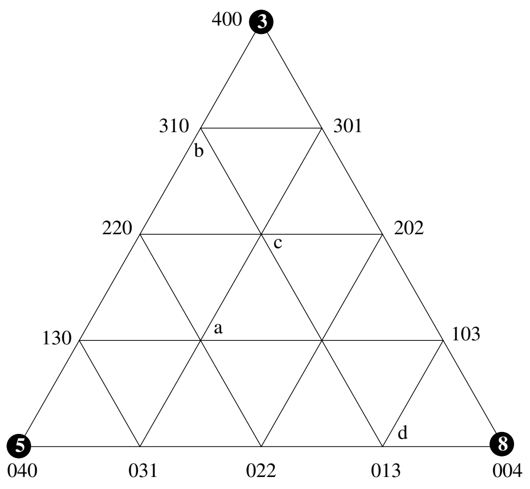

Vertex	Global Barycentric IDs
3	[(0,0),(0,0),(3,4)]
5	[(0,0),(0,0),(5,4)]
8	[(0,0),(0,0),(8,4)]
a	[(3,1),(5,2),(8,1)]
b	[(0,0),(3,3),(5,1)]
c	[(3,2),(5,1),(8,1)]
d	[(0,0),(5,1),(8,3)]

Fig. 4: Integer based barycentric coordinates and global barycentric IDs when two levels of refinement are done on coarse mesh face with vertices 3, 5 and 8

global IDs of some vertices.

Note that even though there are six pieces of information in a barycentric global ID compared with three pieces of information in x, y, z coordinates, storage wise barycentric global IDs are more advantageous. x, y, z coordinates require three doubles (24 bytes). A barycentric coordinate (α or β or γ) can be represented using $r + 1$ bits. The initially generated coarse mesh is small - one or two million at most. A 32 bit unsigned integer is more than enough to fit both the $r + 1$ bits as well as the vertex ID in the coarse mesh. Since we have 3 pairs, 3 unsigned integers, i.e. a total of 12 bytes, are actually sufficient.

We also note that in the literature, applications of barycentric coordinates can be found in many areas such as finite element analysis and computer graphics. Recently in particular, in the area of computer graphics, Boubekeur *et. al* [16, 17] made use of barycentric coordinate based interpolation in generic and adaptive mesh refinement kernels for GPUs. Our use of barycentric global IDs for distributed vertex matching in PMSH is yet another novel application of barycentric coordinates.

In order to compute vertex adjacencies of processors, adjacent processor IDs are inserted into a map whose keys are barycentric global IDs. This is done in step 10. After this step, the fine volume sub-mesh is generated from the fine surface sub-mesh in step 11. OpenFOAM mesh format uses global vertex IDs. Therefore, we need to assign global numbers to all vertices. In steps 12-13, the global numbers of partition boundary vertices are generated by first assigning an owner to one of the processors holding a copy of the vertex. Given a sorted list L of processors that hold a vertex with barycentric global ID $[(i, \alpha), (j, \beta), (k, \gamma)]$ the p^{th} processor in the list is calculated as follows:

$$p = (i + \alpha + j + \beta + k + \gamma) \quad mod \quad |L|$$

Here, $|L|$ is the number of holder processors of the vertex. This method of determining owners is similar to our earlier approach given in [14]. Once owner processors are determined, owner processors generate global numbers for each vertex they own. A pre-scan operation is carried out among processors to compute prefix counts of owned vertices on each processors. From these counts the starting point of global numberings on each processor can be determined. Once global numbers for partition boundary vertices are determined, the owner processors then send these numbers to holder processors in step 14. In this way, all integer global IDs for all vertices (whether they are internal or on partition boundary) are determined. Finally in step 15, the mesh is output in OpenFOAM format using these integer global IDs.

As data structures, Standard Template library (STL) maps are used to store various surface mesh data. The main ones are for the storage of geometry and partition boundary faces, global barycentric IDs of partition boundary vertices and processor adjacencies.

4. Bug Fixes and Modifications Made in Netgen-5.1 code

During the development of this project, Netgen 5.1 was the most recent version. Our modifications and fixes have been made on this version. When we generated fine surface meshes after multiple levels of refinement and passed them to Netgen for fine volume generation (step 11 in the algorithm in Figure 2), we encountered Netgen crashes on a few processors. This happened repeatedly and prevented us from obtaining massive meshes. We examined the Netgen code and traced the bugs. The following fixes as well as some other modifications that let us access some functions within Netgen were made to the Netgen 5.1 code.

1. In `libsrc/meshing/adfront3.cpp`, `points.Get(i).Valid()` was changed to `points[pi].Valid()`. In Netgen-4, the loop index was defined as `i`, but after the loop index was changed to `pi` in Netgen-5.1, this code was not modified and could cause a segmentation fault in some cases.
2. In `libsrc/meshing/improve3.cpp`, on line 1236, `suroundpts[l] = suroundpts[l-1]` was added. In some cases, if the if-clause below this line is not triggered, some elements of the `suroundpts` array may be undefined, which results in Netgen trying to reach a point with a garbage value. This fix avoids this.
3. In `libsrc/interface/nginterface.cpp`, we have added two functions, `Ng_GetElement_Faces` and `writeOF`, which allow us to get the faces and write the mesh in OpenFOAM format using Netgen's nglib library.

The modifications enabled our tests to run successfully. Afterwards, we were able to generate multi-billion element meshes. The bugs we discovered were also reported to the Netgen developer.

5. Tests and Results

We have meshed Onera M6 wing, sphere and shaft geometries shown in Figure 5 on NTNU's Vilje system. Vilje is an SGI Altix ICE X system that has 936 nodes available to academic users. Each node has 2 Intel Xeon E5-2670 (Sandy Bridge) processors with a total of 16 cores and 28 GB of memory. Table 2 shows the results of the mesh generation tests we have performed. On Vilje, due to restrictions, a job can be allocated at most 14.3 TB total memory on up to 512 nodes. Therefore, we submitted tests that would satisfy this memory limit. If this limit was higher, we would have been able to run our tests on higher numbers of cores and generate even bigger meshes than what is shown in Table 2.

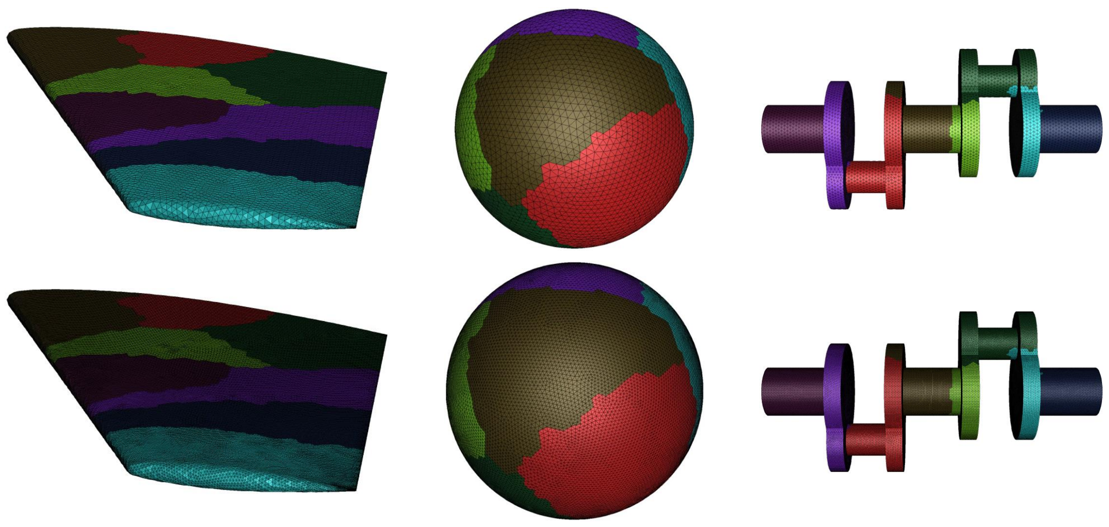

Fig. 5: Test geometries and meshes used: onera-m6.stl (a), sphere.geo (b) and shaft.geo (c). The top picture is the coarse mesh and the bottom one is the (one-level refined) fine mesh

The columns Time taken by coarse mesh $\mathcal{T}$ and fine mesh $\mathcal{T}''$ show the timings of steps 3-4 and steps 5-14 respectively. Total timing is the summation of these two timings. Geometry input and mesh output are not included in the timings. Note that coarse mesh $\mathcal{T}$ is the initial mesh generated on each processor whereas fine mesh $\mathcal{T}''$ is the global mesh over all processors (i.e. union of all $\partial\mathcal{T}_i''$).

When looking at *sequential* mesh generation times of the coarse mesh, we see that on average 0.23 million elements/minute rate is achieved by Netgen. In [3], Löhner states *"Typical speeds for the complete generation of a mesh (surface, mesh, improvement) on current Intel Xeon chips with 3.2 GHz and sufficient memory are of the order of 0.5-2.0 million elements / minute."*. Netgen's meshing rate on a single 2.6 GHz core is lower than this, but still it is a reasonable rate.

When looking at the parallel *multi-billion* element mesh generation results, we see that *within the 1K-8K core range* scalability is achieved. Figure 6 plots mesh generation time curves for $(|\mathcal{T}|, |\mathcal{T}''|)$ pairs. $|\mathcal{T}|$ and $|\mathcal{T}''|$ are the sizes of initial coarse and the final fine mesh respectively. The inputs to our program are the following parameters: (i) maximum element edge length in the mesh, (ii) mesh grading factor between 0.0 and 1.0, and (iii) number of levels of refinement. Parameters $(i)-(ii)$ dictate the size of the coarse mesh and $(i)-(iii)$ dictate the size of the final fine mesh. We can treat coarse and fine mesh sizes, i.e. the pair $(|\mathcal{T}|, |\mathcal{T}''|)$ as our

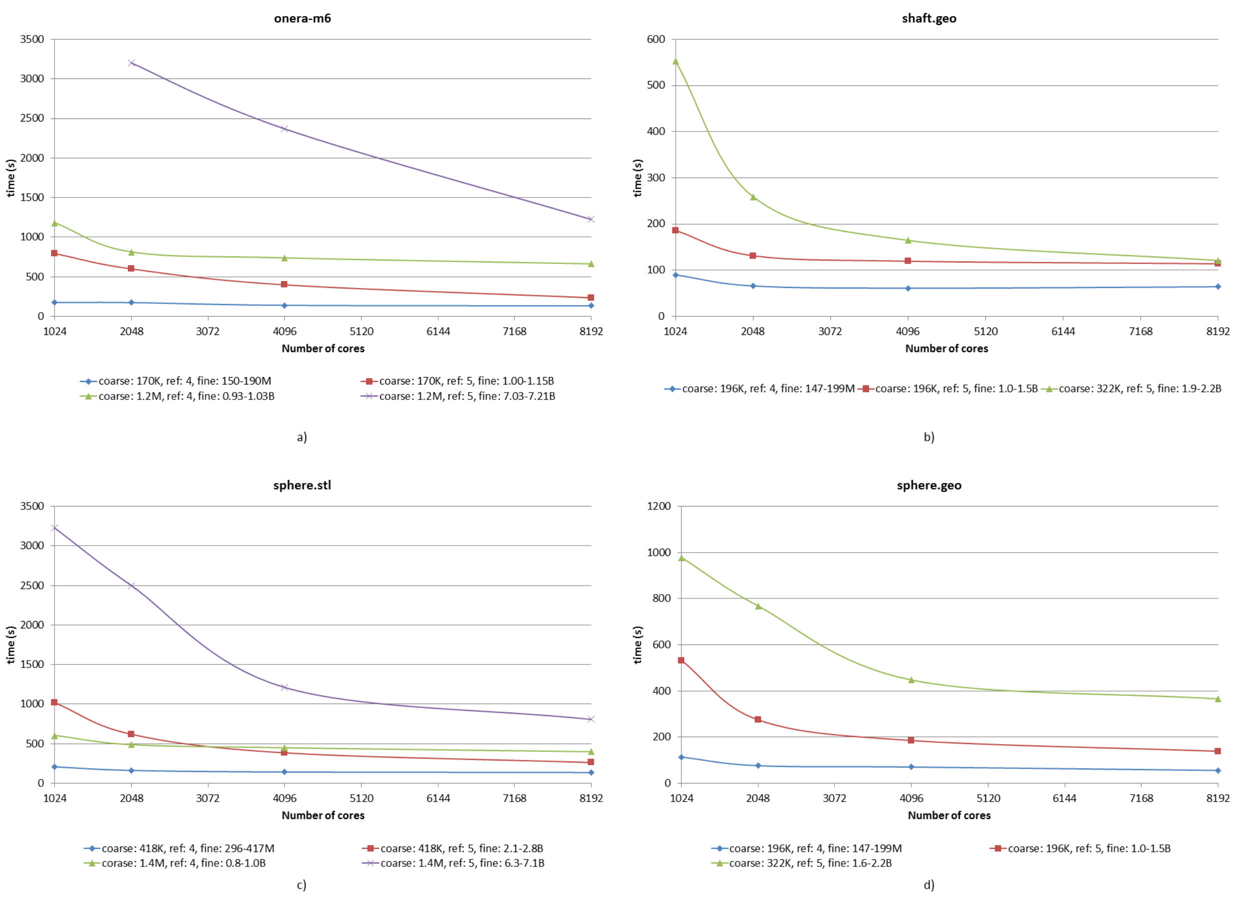

Fig. 6: Parallel mesh generation timings ; for each geometry timings obtained for ranges of $(|\mathcal{T}|, |\mathcal{T}''|)$ pairs are drawn as separate curves

problem size. Since, when changing the number of cores (partitions), the submesh sizes can change (since a new mesh is generated), we have defined ranges on $(|\mathcal{T}|, |\mathcal{T}''|)$ and plotted mesh generation times for ranges of $(|\mathcal{T}|, |\mathcal{T}''|)$. Hence, given a roughly fixed problem size, i.e. a given range of the pair $(|\mathcal{T}|, |\mathcal{T}''|)$, we see from Table 2 that execution times decrease as the number of cores are increased. Of course, as the ratio $|\mathcal{T}''|/P$ gets smaller and smaller, any further increase in the number of cores will lead to smaller and smaller reductions in execution time and will approach the time it takes to generate and partition the coarse mesh.

6. Discussion and Conclusions

We have developed a wrapper tool called PMSH around the existing sequential Netgen mesh generator that enabled us to generate multi-billion element tetrahedral meshes for the OpenFOAM applications. The mesh generation runs on 1K through 8K cores with 14.3 TB total memory limit show that our PMSH implementation scales. Seven billion element meshes that were generated on 8K cores for the Onera M6 wing and the sphere geometries took about 21 minutes and 14 minutes respectively. With a sequential rate of 0.23 million elements/minute, such a mesh would need roughly 21 days to be generated sequentially. It is also interesting to note that by choosing smaller initial coarse meshes, roughly billion element sized meshes can be generated in 2-4 minutes.

The PMSH tool code is maintained at https://code.google.com/p/pmsh/. Our future work will focus on the development of a malleable parallel mesh generation system and implementation of more advanced schemes for projecting vertices on geometric boundaries.

Acknowledgements

This work was financially supported by the PRACE-3IP project funded in part by the EUs 7th Framework Programme (FP7/2012-2014) under grant agreement no. RI-312763. We thank Peter Stadelmeyer for initial discussions that motivated the development of this tool. We also acknowledge greatly Vilje supercomputer allocation provided to us by NTNU and the always prompt helps we received from Bjorn Lindi on the use of Vilje system. Finally, we thank Mustafa Dindar for providing us with Onera M6 wing geometry in STL format.

Table 2: Mesh generation results

	Number	Allocated Job	Refinement	Mesh Size (M)		Time Taken by (s)		
Geometry	**of Cores**	**Memory (TB)**	**Levels (r)**	**Coarse $\mathcal{T}$**	**Fine $\mathcal{T}''$**	**Coarse $\mathcal{T}$**	**Fine $\mathcal{T}''$**	**Total**
oneram6.stl	1024	7.2	4	0.2	156.1	78.95	96.08	175.03
	2048	14.3	4	0.2	174.8	78.93	95.38	174.31
	4096	14.3	4	0.2	183.1	85.67	55.16	140.83
	8192	14.3	4	0.2	189.6	81.97	51.27	133.24
	1024	7.2	5	0.2	1014.7	78.96	715.3	794.26
	2048	14.3	5	0.2	1114.3	78.89	521.68	600.57
	4096	14.3	5	0.2	1123.3	82.73	316.04	398.77
	8192	14.3	5	0.2	1152.7	82.14	152.66	234.8
	1024	7.2	4	1.2	929.5	483.15	700.91	1184.06
	2048	14.3	4	1.2	970.9	482.69	331.96	814.65
	4096	14	4	1.2	909.1	537.04	202.96	740
	8192	14	4	1.2	1028.9	510.94	152.93	663.87
	2048	14.3	5	1.2	7030.7	483.16	2719.29	3202.45
	4096	14	5	1.2	6393.5	538	1831.23	2369.23
	8192	14	5	1.2	7209.8	510.59	713.66	1224.25
sphere.geo	2048	14.3	5	0.3	1773.3	184.42	583.59	768.01
	4096	14.3	5	0.3	2134.4	242.52	204.96	447.48
	8192	14.3	5	0.3	2163.3	232.15	133.28	365.43
	1024	7.2	5	0.3	1625.5	181.18	796.93	978.11
	1024	7.2	4	0.2	146.7	43.88	69.72	113.6
	2048	14.3	4	0.2	176.7	44.01	32.32	76.33
	4096	14.3	4	0.2	198.7	47.02	23.6	70.62
	8192	14.3	4	0.2	217	45.04	10.8	55.84
	1024	7.2	5	0.2	1048.4	43.95	488.25	532.2
	2048	14.3	5	0.2	1278.4	44.02	230.87	274.89
	4096	14.3	5	0.2	1367.6	47	138.46	185.46
	8192	14.3	5	0.2	1476.7	46.74	92.01	138.75
sphere.stl	1024	7.2	4	1.4	829.5	286.32	319.88	606.2
	2048	14.3	4	1.4	931.4	286.96	201.49	488.45
	4096	14.3	4	1.4	900.4	299.03	150.31	449.34
	8192	14.3	4	1.4	1001.5	294.21	105.18	399.39
	1024	7.2	4	0.4	296.4	94.13	114.04	208.17
	2048	14.3	4	0.4	301.6	93.81	69.17	162.98
	4096	14.3	4	0.4	365.4	97.91	45.35	143.26
	8192	14.3	4	0.4	417.4	96.31	40.41	136.72
	1024	7.2	5	1.4	6392.3	286.51	2938.7	3225.21
	2048	14.3	5	1.4	6847.5	286.88	2212.16	2499.04
	4096	14.3	5	1.4	6283.1	298.83	912.7	1211.53
	8192	14.3	5	1.4	7053.6	293.56	513.41	806.97
	1024	7.2	5	0.4	2120	94	924.97	1018.97
	2048	14.3	5	0.4	2131.1	93.76	525.56	619.32
	4096	14.3	5	0.4	2584.5	97.82	287.31	385.13
	8192	14.3	5	0.4	2840.7	96.59	166.04	262.63
shaft.geo	1024	7.2	4	0.2	139.6	37.37	52.55	89.92
	2048	14.3	4	0.2	166.8	37.4	28.61	66.01
	4096	14.3	4	0.2	182.5	39.01	22.11	61.12
	8192	14.3	4	0.2	221.4	38.42	25.73	64.15
	1024	7.2	4	0.4	281.4	75.21	110.85	186.06
	2048	14.3	4	0.4	295.6	75.7	55.71	131.41
	4096	14.3	4	0.4	351.7	78.87	40.67	119.54
	8192	14.3	4	0.4	382.2	77.74	36.23	113.97
	1024	7.2	5	0.2	948.4	37.38	515.95	553.33
	2048	14.3	5	0.2	1139.9	37.47	221.87	259.34
	4096	14.3	5	0.2	1191.5	39	125.79	164.79
	8192	14.3	5	0.2	1340.3	38.42	82.55	120.97
	1024	7.2	5	0.4	1991.3	75.21	920.31	995.52
	2048	14.3	5	0.4	2081.9	75.37	486.93	562.3
	4096	14.3	5	0.4	2475.1	78.81	260.88	339.69
	8192	14.3	5	0.4	2568.2	77.84	168.31	246.15

References

1. OpenFoam. `http://www.openfoam.org/`.
2. J. Schöberl. Netgen an advancing front 2d/3d-mesh generator based on abstract rules. *Computing and visualization in science*, 1(1):41–52, 1997.
3. Rainald Löhner. Recent advances in parallel advancing front grid generation. *Archives of Computational Methods in Engineering*, pages 1–14, 2014.
4. J. Bell L Chacon R. Falgout M. Heroux P. Hovland E. Ng C Webster S. Wild J. Dongarra, J Hittinger. *Applied mathematics research for exascale computing report.*
5. WN Dawes, SA Harvey, Simon Fellows, Neil Eccles, D Jaeggi, and WP Kellar. A practical demonstration of scalable, parallel mesh generation. In *47th AIAA Aerospace Sciences Meeting & Exhibit*, pages 5–8, 2009.
6. A. Chernikov F. Blagojevic and D. Nikolopoulos. A multigrain delaunay mesh generation method for multicore smt-based architectures. *Journal of Parallel and Distributed Systems*, 69(7):589–600, 2009.
7. D3D mesh generator. `http://mech.fsv.cvut.cz/~dr/d3d.html`.
8. MeshSim, Simmetrix inc. `http://www.simmetrix.com`.
9. E Ivanov, O Gluchshenko, H Andrä, and A Kudryavtsev. Parallel software tool for decomposing and meshing of 3d structures. 2007.
10. Pamgen Mesh Generation. `http://trilinos.sandia.gov/packages/pamgen/`, 2014.
11. M. Vazquez G. Houzeaux, R. de la Cruz. Parallel uniform mesh subdivision in alya. *PRACE project (FP7/2007-2013)*, 2011.
12. P. Kabelikova, A. Ronovsky, and V. Vondrak. Parallel mesh multiplication for code saturne. *PRACE project (FP7/2007-2013)*, 2011.
13. V. Vondrak C. Moulinec A. Ronovsky, P. Kabelikova. Parallel mesh multiplication and its implementation in code saturne. In *Proc. of the Third International Conference on Parallel, Distributed, Grid and Cloud Computing for Engineers*. Civil-Comp Press, 2013.
14. Y. Yilmaz, C. Ozturan, O. Tosun, A. H. Ozer, and S. Soner. Parallel mesh generation, migration and partitioning for the elmer application. *PRACE project (FP7/2007-2013)*, 2011.
15. G. Karypis and V. Kumar. A fast and high quality multilevel scheme for partitioning irregular graphs. *SIAM Journal on scientific Computing*, 20(1):359–392, 1998.
16. T. Boubekeur and C. Schlick. Generic mesh refinement on gpu. In *Proceedings of the ACM SIGGRAPH/EUROGRAPHICS conference on Graphics hardware*, pages 99–104. ACM, 2005.
17. T. Boubekeur and C. Schlick. A flexible kernel for adaptive mesh refinement on gpu. In *Computer Graphics Forum*, volume 27, pages 102–113. Wiley Online Library, 2008.